Ergodic Hysteresis of the Kerr black hole spectrum

João Paulo Cavalcante, ^{1,*} Maurício Richartz, ^{1,†} and Bruno Carneiro da Cunha^{2,‡}

¹ Centro de Matemática, Computação e Cognição,
Universidade Federal do ABC (UFABC), 09210-580, Santo André, São Paulo, Brazil

² Departamento de Física, Universidade Federal de Pernambuco, 50670-901, Recife, Brazil

We uncover a cascade of exceptional points (EPs) in the quasinormal mode spectrum of massive scalar perturbations of Kerr black holes, revealing an intricate non-Hermitian structure underlying their linear response. The cascade originates from a single damped mode that enters the extremal spectrum for sufficiently large field masses. We obtain evidence for an infinite sequence of EPs in the $(\ell, m) = (1, 1)$ and (2, 2) sectors near the extremal limit, mediating the transition between damped and zero-damping modes. Each EP carries a geometric phase that enables adiabatic mode mixing across the entire overtone spectrum, a phenomenon we refer to as adiabatic ergodicity.

Introduction - Quasinormal modes (QNMs), and their associated complex frequencies ω , characterize the damped oscillations through which systems, ranging from black holes to vortex flows, respond to external perturbations and lose energy [1–9]. In gravitational systems, QNMs may be excited, for instance, through test fields [10, 11], infalling particles [12], and mergers [13]. In vaccum General Relativity, QNM frequencies for each set of mode numbers (ℓ, m, n) depend only on the mass M and the spin a of the black hole, thereby providing the basis for black hole spectroscopy [14–16]. An interesting feature of the QNM spectrum emerges as the extremal limit $(a \to M)$ is approached [17, 18]. In this regime, the spectrum branches into zero-damping modes (ZDMs) and damped modes (DMs). ZDMs are characterized by $\omega \to m/(2M)$ and a vanishing imaginary part as $a \to M$. Unlike DMs, these modes are long-lived in the extremal limit and play a crucial role in analyses of black hole stability [19–26].

The eigenvalue problem underlying black hole perturbations is non-Hermitian. Hence, eigenvalue degeneracies that manifest as exceptional points (EPs) are, in principle, permitted [27, 28]. Such EPs give rise to remarkable phenomena across different areas of physics, including spectral sensitivity [29] and geometric phases [30]. Although the study of EPs in gravitational physics is still incipient, recent work [31–36] has begun to connect black hole perturbations to the rich EP phenomenology observed in open quantum systems [37], condensed matter [38], and photonics [39]. In particular, QNMs of a massive scalar field around a near extremal Kerr black hole may coalesce, revealing hysteretic behavior when the associated EP is adiabatically encircled in parameter space [35, 36].

Expanding on these developments, Ref. [40] analyzed EPs (and avoided crossings) in the Kerr and Kerr—de Sitter spectrum. It was shown that, while mode amplitudes can be resonantly enhanced near EPs, modes undergoing avoided crossings interfere destructively, preserving the stability of the ringdown signal. Ref. [41] conducted a numerical study of resonances between the fundamental mode and the first overtone in a simplified model, provid-

ing further evidence of EP behavior and demonstrating that QNM frequencies cannot be accurately constrained without accounting for resonance effects. Ref. [42], working with a novel method to determine QNMs of Type-D black holes, confirmed the existence of an EP between the n=0 and n=1 modes for massive perturbations of Kerr black holes, corroborating previous findings. Ref. [43], on the other hand, used a two-level effective Hamiltonian to demonstrate that crossings in the real parts of QNM frequencies coincide with avoided crossings in the imaginary parts, with resonant effects strongest near an EP.

In this Letter, we investigate the structure of EPs in the QNM spectrum of massive scalar perturbations around Kerr black holes. We find an infinite sequence of EPs associated with $(\ell, m) = (1, 1)$ and (2, 2) modes. In particular, the geometric phases that arise around each EP enable an adiabatic mixing of the entire spectrum of overtones under closed variations of the system parameters. We also examine the role of EPs in mediating the transition between DMs and ZDMs. By carefully tracking the relevant QNM branches as the parameters are varied, we trace the origin of the EPs, and their associated geometric phases, to a single DM that enters the extremal spectrum for sufficiently large values of the scalar field mass μ . Finally, we propose a simple technique to count the number of EPs in a given black hole system without the need to explicitly identify the underlying degeneracies.

Throughout this work we adopt natural units $(G = c = \hbar = 1)$.

QNM problem via the Isomonodromic method — Recent developments in the theory of the differential equations governing quasinormal modes have emphasized the key role of the global analytic structure of the solutions. This structure is best framed in terms of the monodromy parameters, which, for second order differential operators with algebraic potentials, can be related to quantum periods of the Seiberg-Witten curve used in certain four-dimensional supersymmetric field theories [44–46]. This relation led to connection formulas for the Heun equation and its confluent limits [47, 48], as well as explicit series solutions for the Jimbo-Miwa-Ueno tau func-

tion of isomonodromic deformations [49–54]. The latter has enabled efficient numerical computation of QNMs in a variety of black holes [55–64].

In the case of massive scalar perturbations around Kerr black holes, suitable changes of variables reduce both the radial and angular wave equations to the confluent Heun equation (CHE) [36]

$$\frac{d^2y}{dz^2} + \left[\frac{1-\theta_1}{z} + \frac{1-\theta_2}{z-t}\right] \frac{dy}{dz} - \left[\frac{1}{4} + \frac{\theta_*}{2z} + \frac{t c_t}{z(z-t)}\right] y = 0.$$
(1)

For the radial equation, the monodromy parameters $\{\theta_1, \theta_2, \theta_{\star}\}$, together with the accessory parameter c_t and the modulus t, are given by [36]

$$\theta_{1} = \frac{-i}{2\pi T_{-}} \left(\omega - m\Omega_{-}\right), \quad \theta_{2} = \frac{i}{2\pi T_{+}} \left(\omega - m\Omega_{+}\right),$$

$$\theta_{\star} = \frac{2iM(2\omega^{2} - \mu^{2})}{\sqrt{\omega^{2} - \mu^{2}}}, \quad t = 2i(r_{+} - r_{-})\sqrt{\omega^{2} - \mu^{2}}, \quad (2)$$

$$tc_{t} = \lambda_{\ell,m} + r_{+}^{2}\mu^{2} - (3a^{2} + r_{-}^{2} + 3r_{+}^{2})\omega^{2} + \frac{1}{2}t(\theta_{2} - 1) - \frac{1}{4}(\theta_{\star} - 2)\theta_{\star},$$

where $\lambda_{\ell,m}$ is the angular eigenvalue and r_{\pm} denotes the Cauchy (-) and event (+) horizons, with corresponding temperatures and angular velocities given by $T_{\pm} = (r_{+} - r_{-})/(8\pi M r_{\pm})$ and $\Omega_{\pm} = a/(2M r_{\pm})$, respectively.

This framing of the QNM eigenvalue problem allows the exploration of the spectrum across the entire parameter space, covering both the Schwarzschild and extremal limits, as is described in detail in [35]. The relevant Julia scripts are made publicly available in [65]. Concretely, the isomonodromic method solves the Riemann-Hilbert map, which relates the monodromy properties of solutions of the generic CHE equation (1) to its parameters. The non-trivial monodromy data consists of two complex parameters σ, η , and the map is achieved by simultaneously solving two transcendental equations

$$\tau_{V}(\theta_{1}, \theta_{2}, \theta_{\star}; \sigma, \eta; t) = 0, \quad (3a)$$

$$\frac{d}{dt} \log \tau_{V}(\theta_{1}, \theta_{2} - 1, \theta_{\star} + 1; \sigma - 1, \eta; t) - \frac{\theta_{1}(\theta_{2} - 1)}{2t} = c_{t},$$
(3b)

where τ_V is the tau function for the Painlevé V transcendent. General expansions of τ_V for small t have been given by [54, 66] in terms of Nekrasov functions. A Fredholm determinant formulation was derived in [66] and adapted to QNM problems in [58]. In the isomonodromic method, the QNM boundary conditions translate into the following relation between the parameters σ and η (valid for Re $(M\omega) > m/2$),

$$e^{\pi i(\eta + \sigma)} = \frac{\sin\frac{\pi}{2}(\theta_{\star} + \sigma)}{\sin\frac{\pi}{2}(\theta_{\star} - \sigma)} \prod_{\epsilon = \pm 1} \frac{\sin\frac{\pi}{2}(\theta_{2} + \epsilon\theta_{1} + \sigma)}{\sin\frac{\pi}{2}(\theta_{2} + \epsilon\theta_{1} - \sigma)}.$$
 (4)

We remark that, when the black hole is extremal, the radial wave equation for massive scalar perturbations reduces to the double-confluent Heun equation (DCHE) rather than the CHE. The Riemann-Hilbert map (3) for the DHCE is expressed in terms of the Painlevé III tau function [61]. Details relevant to the present discussion are provided in the Supplemental Material.

\overline{n}	$(M\mu)_n^c$	$(a/M)_n^c$	n	$(M\mu)_n^c$	$(a/M)_n^c$
0	0.37049813	0.99946597	7	0.23336824	0.99999142
1	0.31913513	0.99985379	8	0.22797842	0.99999328
2	0.29034662	0.99993511	9	0.22342370	0.99999460
3	0.27150936	0.99996399	10	0.21951655	0.99999556
4	0.25805197	0.99997729	11	0.21612255	0.99999629
5	0.24787479	0.99998443	12	0.21314391	0.99999686
6	0.23986499	0.99998869	13	0.21050463	0.99999730

TABLE I. The first 14 EPs for $(\ell,m)=(1,1)$ massive scalar perturbations of Kerr black holes. The critical values $(M\mu)_n^c$ and $(a/M)_n^c$ are determined by numerically solving Eq. (3). The associated QNM frequencies, which are doubly degenerate, are shown in Fig. 1.

Numerical Results and EP Cascade – In previous work [35, 36], we determined the existence of an EP in the QNM spectrum of massive scalar perturbations around near extremal Kerr black holes, which characterizes an accidental degeneracy between the fundamental mode and the first overtone. This EP also signals a transition where the fundamental mode changes from ZDM to DM as $M\mu$ increases. A natural question that follows is how unique this EP is and how general such transitions are.

By exploring the parameter space in greater detail, we find a series of EPs that sheds light on these issues. Each EP is associated with the degeneracy of a pair of two subsequent overtones (n, n+1) and has a corresponding geometric phase. We characterize each EP by the index n of the lowest associated overtone, so that the corresponding critical parameter for the scalar mass and spin are denoted, respectively, by $(M\mu)_n^c$ and $(a/M)_n^c$. In Table I, we exhibit the first 14 EPs for $(\ell, m) = (1, 1)$, which mix the (n, n+1) pair of overtones up to n=13.

To each EP there is a corresponding ZDM to DM transition, and a parametric plot of the various transitions can be seen in Fig. 1. The EPs form what we refer to as a degeneracy cascade. The solid (red) lines, which spiral towards the extremal limit, correspond to DMs. On the other hand, the ZDM behavior is represented by the dashed (black) lines, which can be seen to converge to the asymptotic value $M\omega = m/2 = 1/2$ as the extremal limit is approached. Additionally, given the associated geometric phases, the two overtones related to a given EP can be transformed into each other if the system parameters are adiabatically varied along a sufficiently small curve around the EP, generalizing the hysteresis phenomenon first revealed in [36]. Note that each overtone n may become degenerate with respect to its two

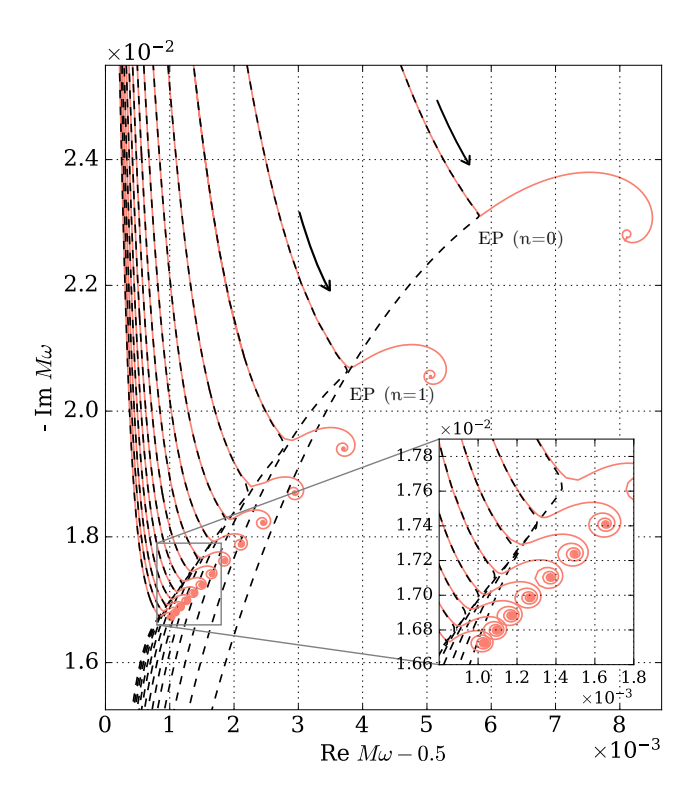


FIG. 1. The behavior of the $(\ell,m)=(1,1)$ overtones, parametrized by a/M, near the associated EPs. Each dashed curve corresponds to a fixed scalar mass $M\mu\lesssim (M\mu)_n^c$, while each solid curve corresponds to $M\mu\gtrsim (M\mu)_n^c$. For $a/M<(a/M)_n^c$, the curves are indistinguishable. As the black hole spin increases (along the direction of the arrow), the EP is reached and the initially coincident curves branch out. Dashed curves are ZDMs, which approach $\mathrm{Im}\,(M\omega)=0$ as $a/M\to 1$. Solid curves are DMs, which spiral to a finite decay time in the extremal limit.

neighboring modes $(n \pm 1)$ and is, therefore, directly associated with two EPs. Since each EP marks a ZDM to DM transition, this implies the existence of a window $(M\mu)_{n+1}^c < M\mu < (M\mu)_n^c$ in which the *n*-th overtone is a DM for $a/M \to 1$ (i.e. $r_+ \to r_-$), as illustrated in Fig. 2 for n = 3.

An analytical description of the QNMs around an EP can be obtained from the transcendental equations (3), since the QNM problem is equivalent to solving a nonlinear secular equation $\det(\mathbb{1}-\mathsf{K}(\omega))=0$ [35]. The integral operator K is given explicitly in [58]. Each EP, characterized by the degeneracy of two QNMs, corresponds to a double root of the secular equation. Assuming analiticity of the operator K with respect to a/M and $M\mu$, the eigenvalue difference near the n-th EP is given, to lowest order, by (see the Supplemental Material for details)

$$((M\omega)_{n+1} - (M\omega)_n)^2 \approx A_n((a/M) - (a/M)_n^c) + B_n((M\mu) - (M\mu)_n^c), \quad (5)$$

where A_n and B_n are expansion coefficients. Table II

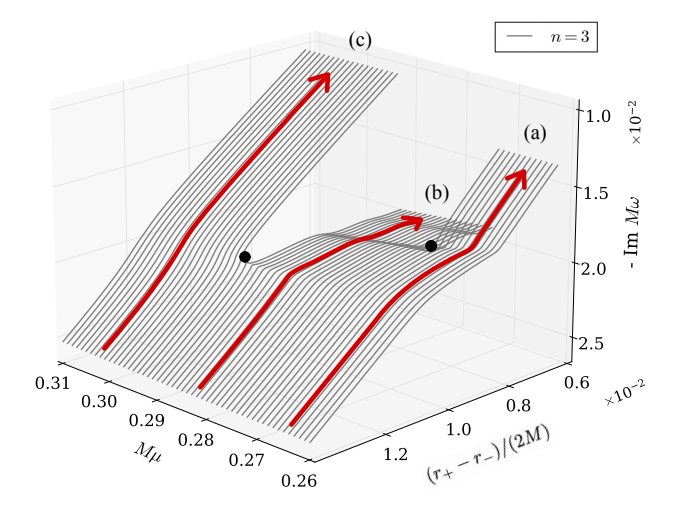


FIG. 2. The near-extremal behavior of the n=3 QNM across a range of $M\mu$ encompassing the n=2 and n=3 EPs (denoted by dots). The mode transitions from ZDM to DM at each EP. Within region (b), corresponding to the window $(M\mu)_3^c < (M\mu) < (M\mu)_2^c$, the n=3 mode exhibits DM behavior, whereas in regions (a) and (c) it behaves as a ZDM.

\overline{n}	$A_n \times 10^{-3}$	B_n
0	1.190202 - 0.800304i	0.104888 - 0.393782i
1	0.502592 - 0.416007i	0.139330 - 0.723933i
2	0.289935 - 0.264467i	0.160232 - 1.047625i
3	0.194913 - 0.188481i	0.175178 - 1.368997i
4	0.143415 - 0.144198i	0.186790 - 1.689281i
5	0.111897 - 0.115722i	0.196266 - 2.008970i

TABLE II. Complex expansion coefficients A_n and B_n , as defined in (5), associated with the first six EPs.

lists the numerical values of A_n and B_n for the first six EPs, obtained by fitting the above expression to QNM data. These results extend and confirm the findings of Ref. [41] on the complex square-root behavior near an EP. We point out, as discussed in the Supplemental Material, that A_n has roughly the behavior of an harmonic series in n, evidence for an infinite number of EPs.

QNMs: from Schwarzschild to extremal Kerr – At any fixed point in the parameter space $(a/M, M\mu)$, the ordering of the QNM spectrum is unambiguous. One first determines the spectrum by solving the radial and angular equations together, and then orders the modes by the magnitude of the imaginary part of their frequencies. However, the existence of EPs and the associated geometric phases makes such an ordering considerably less robust. As shown in [36], different adiabatic paths can yield different final states, and a single turn around the EP interchanges adiabatically the two levels involved in the accidental degeneracy. The cascade consisting of multiple (possibly infinitely many) EPs allows a complete

mixture of the spectrum, as we explain below.

When the scalar field is massless, all $(\ell, m) = (1, 1)$ modes of the Kerr spectrum are ZDMs [35, 36]. The spectrum of ZDMs in the extremal regime $a/M \to 1$, indexed by $k \in \mathbb{N}$, is given by [35, 67]

$$\omega_k \simeq \frac{1}{2M} - i2\pi T_+ \left(k + \frac{1}{2}\right) - i\pi T_+ \sqrt{4\lambda_0 + 4M^2\mu^2 - 6},$$

where $\lambda_0 = (4M^2\mu^2 + 39)/20$ (see also [22, 23, 60, 68– 70]). Since EPs mark transitions between ZDMs and DMs, we expect DMs to emerge in the spectrum if $M\mu$ is sufficiently large. In fact, we have confirmed that for sufficiently low masses $M\mu < (M\mu)^c_{\star}$, where $(M\mu)^c_{\star} \approx$ 0.16188, the near extremal Kerr spectrum is comprised only by ZDMs for $(\ell, m) = (1, 1)$. At $(M\mu)^c_{\star}$, we note the appearance of a single damped mode in the extremal spectrum, with frequency $(M\omega)^c_{\star} \approx 0.50000 - 0.015490i$. We defer the technical details for the Supplemental Material, but, as explained below, we confirmed that it belongs to the spectrum by following it adiabatically in parameter space. By tracking this DM along the extremal line a/M = 1, we determined that it remains part of the spectrum for at least $(M\mu)_{\star}^{c} \leq M\mu \leq M\mu_{max}$. The value $M\mu_{max} \approx 0.8705$ reflects a limitation of the condition (24), as explained in [35], which is not relevant for the present discussion. The behavior of the DM at extremality (a/M = 1) is shown in Fig. 3.

We follow the DM adiabatically along a path that starts at the line a/M=1 and ends at the origin $(a/M, M\mu)=(0,0)$. Because EPs are present, the outcome depends not only on the choice of the starting point but also on the path itself. For definiteness, we adopt the trajectory DEFA shown in Fig. 4. We first lower the spin from a/M=1 to a/M=0.99 while keeping $M\mu=(M\mu)|_D$ fixed. Next, we decrease the mass $M\mu$ to zero, at fixed a/M. Finally, we reduce a/M to zero, keeping $M\mu=0$, and thus reach the origin. The resulting mode is then compared against the Schwarzschild overtone spectrum, allowing us to associate each starting value $(M\mu)|_D$ with the appropriate overtone number n.

We find that this procedure yields arbitrarily large values of n as $(M\mu)|_D$ approaches (from above) the critical mass $(M\mu)^c_{\star}$. This is another evidence for the presence of an infinite sequence of EPs, following the cascade shown in Fig. 1, which accumulate at the point $(a/M, M\mu) = (1, (M\mu)^c_{\star})$. In contrast, increasing the initial value of $(M\mu)|_D$ decreases the overtone number n obtained at the end of the procedure. For example, if the starting mass lies in the interval $(M\mu)^c_3 \leq (M\mu)|_D < (M\mu)^c_2$ (see the shaded band in Fig. 3), the procedure yields n=3. If the initial mass satisfies $(M\mu)|_D \geq (M\mu)^c_0$, it returns the fundamental mode n=0. Hence, we conclude that the geometric phases associated with EPs are ergodic: any value of n can be retrieved in the massless Schwarschild case by suitably choosing the initial scalar mass value at

extremal spin as $(M\mu)_n^c \leq (M\mu)|_D < (M\mu)_{n-1}^c$.

Ergodic hysteresis and EP counting – Evidence for an infinite EP cascade, together with the ergodicity of the associated geometric phases, leads to the notion of ergodic hysteresis: any state at a fixed point in the parameter space $(a/M, M\mu)$ can be adiabatically connected to any other state at the same point, provided the chosen path encloses a suitable combination of EPs. For example, starting from the fundamental QNM at $(a/M, M\mu) = (0,0)$, if one adiabatically follows a path that encloses the first n EPs and returns to the origin, the system ends up in the nth overtone rather than the fundamental mode. Even if the precise locations of the EPs are unknown, this mechanism offers a way to determine how many of them lie inside a given closed path.

To illustrate ergodic hysteresis and the EP counting strategy, we use the case $(\ell, m) = (2, 2)$ as an example. Starting at the origin of the parameter space, we track how the fundamental mode changes as we follow the closed contour ABCDEFA around the shaded region shown in Fig. 4. This region is bounded from above by the curve BC along which the fundamental mode has $\operatorname{Im}(M\omega) = 0$, extending from $(a/M, M\mu) \simeq (0, 0.821)$ to (1, 1.476). Along the extremal line a/M = 1, the spectrum exhibits a single DM for 1.114 $\lesssim M\mu \lesssim$ 1.476. We fix $(a/M)|_E = (a/M)|_F = 0.99$ and vary $(M\mu)|_{D} = (M\mu)|_{E}$, so the trajectory DEF determines how many EPs are enclosed by the loop. For instance, when $(M\mu)|_D = 1.170$, the mode obtained after completing the loop no longer corresponds to the fundamental mode, but instead to the first overtone. In this case, the trajectory encloses a single EP where these two modes coalesce. We estimate the location of this degeneracy to be approximately $(a/M, M\mu) \simeq (0.9999, 1.1717)$. More generally, as shown in Table III, different choices of $(M\mu)|_D$ result in different overtones after completing the loop, allowing us to infer how many EPs are enclosed. For example, choosing $(M\mu)|_{D} = 1.1200$ yields the 26-th overtone, implying 26 EPs within the path. As $(M\mu)|_D$ approaches the critical value $(M\mu)^c_{\star} \simeq 1.114$, the overtone number increases significantly $(n \gg 1)$, enabling the inference of n (and thus the number of EPs) through the asymptotic formula of [71] (or its generalizations [72–74]).

$M\mu$	n	$M\omega_n$	$(M\mu) _D$	n	$M\omega_n$
1.1450	2	0.43054 - 0.50855i	1.1275	9	0.27146 - 2.23933i
1.1400	3	0.39386 - 0.73809i	1.1250	12	$0.24547 - 2.99854\mathrm{i}$
1.1350	5	0.33489 - 1.22841i	1.1225	16	0.22258 - 4.00841i
1.1300	7	0.29697 - 1.73276i	1.1200	26	0.18979 - 6.52486i

TABLE III. Mapping of the fundamental QNM to the *n*th overtone after one loop around the path ABCDEFA in Fig. 4, which begins and ends at the origin $(a/M, M\mu) = (0, 0)$. The value of $(M\mu)|_D = (M\mu)|_E$ determines the final frequency and, therefore, the number of EPs enclosed by the path.

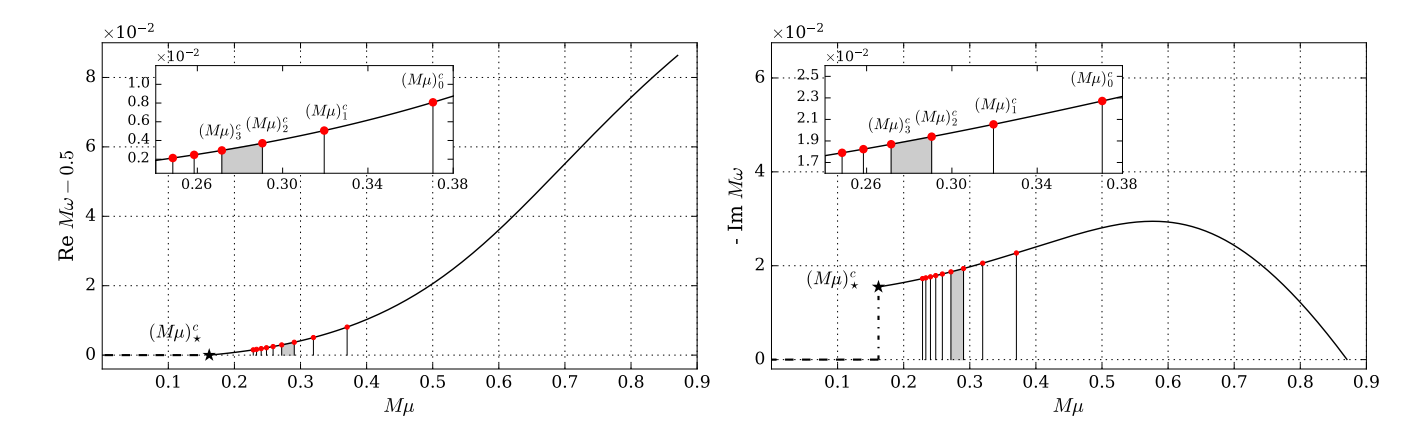


FIG. 3. The real (left) and imaginary (right) parts of the DM frequency as functions of $M\mu$ in the extremal regime a/M=1 are shown by the solid curve originating at the star. The star marks the frequency associated with the lowest scalar mass for which this DM exists, namely $M\mu = (M\mu)_{\star}^c \simeq 0.16189$. Red dots denote the DM frequencies at a/M=1 and $M\mu = (M\mu)_n^c$. The shaded band corresponds to the interval $(M\mu)_3^c < M\mu < (M\mu)_2^c$, which partially overlaps with region (b) of Fig. 2. Vertical lines illustrate how the spacing between EPs progressively narrows as one approaches the critical point $(M\mu)_{\star}^c \simeq 0.16189$, signaling the termination of the EP cascade. For visual clarity, we display only the first nine red dots.

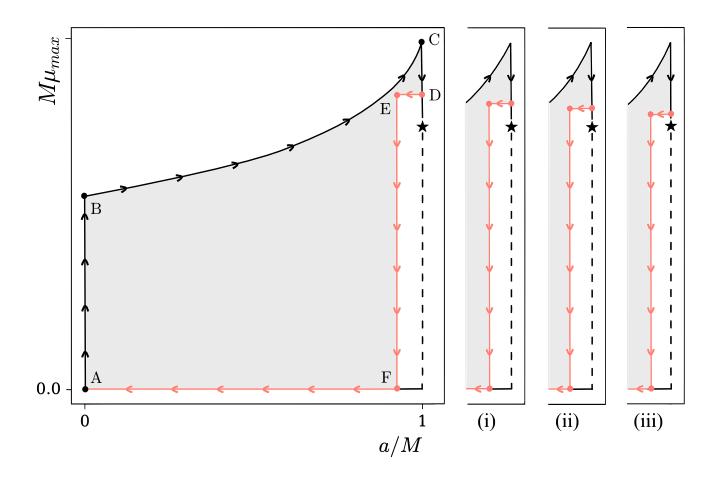


FIG. 4. The closed path ABCDEFA around the shaded region, beginning and ending at the origin, along which we adiabatically track the evolution of the Schwarzschild fundamental mode. The trajectories labeled (i), (ii), and (iii) illustrate different choices of $(M\mu)|_D = (M\mu)|_E$, each enclosing a different number of EPs within the shaded region.

Discussion – We presented evidence above for infinite EP cascades in the $(\ell,m)=(1,1)$ and (2,2) sectors of the Kerr QNM spectrum of massive scalar perturbations, arising in the near-extremal regime through ZDM–DM transitions induced by accidental degeneracies. The associated geometric phases mix in such a way that, by choosing an appropriate path in parameter space, any two QNMs at arbitrary points can be connected adiabatically, a phenomenon we refer to as adiabatic ergodicity. Given the structure revealed for $(\ell,m)=(1,1)$ and (2,2), we expect EP cascades and adiabatic ergodicity to arise

throughout the entire $m \geq 1$ spectrum. Our findings reinforce the emerging view of rotating black holes as natural laboratories for non-Hermitian physics and EP dynamics.

In particular, the existence of an infinite number of EPs raises the intriguing possibility of EP-based mode control in black hole dynamics. During a ringdown phase dominated by the lowest overtones, adiabatic evolution of the system parameters along a path enclosing several points of an infinite EP cascade could, in principle, redistribute energy among overtones in a controlled manner, exciting higher modes while de-exciting lower ones. Whether such behavior can occur dynamically in black holes is an open question. Notably, in photonics and optomechanics, mode and energy manipulation through EP encirclement is already an active area of research [75–81], suggesting nontrivial gravitational analogs yet to be explored.

 ${\it Data~Availability}$ – Data supporting the findings of this work are available from the authors upon reasonable request.

Acknowledgements – The authors thank J. Barragán-Amado for comments and suggestions on the manuscript. J. P. C. acknowledges the financial support from the São Paulo Research Foundation (FAPESP, Brazil), Process Number 2024/15921-9. M. R. acknowledges partial support from the Conselho Nacional de Desenvolvimento Científico e Tecnológico (CNPq, Brazil), Grant 315991/2023-2, and from the São Paulo Research Foundation (FAPESP, Brazil), Grant 2022/08335-0.

SUPPLEMENTAL MATERIAL

The spectrum near EPs – The Riemann-Hilbert map (3), along with the Fredholm determinant formulation of the Painlevé tau functions, casts the equations satisfied by the QNMs into a type of non-linear secular equation. This was pointed out in [35], and the procedure is as follows. The accessory parameter c_t has an expansion in terms of the modulus t:

$$c_t = c_{-1}(\sigma)t^{-1} + c_0(\sigma) + c_1(\sigma)t + \dots,$$
 (7)

where we have omitted the dependence of the coefficients c_k on the single monodromy parameters $\{\theta_k\} = \{\theta_1, \theta_2, \theta_{\star}\}$. The explicit formula can be obtained, for instance, using the continued fraction method of [63]. This expansion can be formally inverted as

$$\sigma = \sigma_0 + \sigma_1 t + \sigma_2 t^2 + \dots, \tag{8}$$

with the coefficients σ_k given by rational functions of θ_1 and θ_2 , and polynomials in θ_{\star} and c_t . The first two terms are

$$\sigma_0 = \theta_1 + \theta_2, \quad \sigma_1 = \frac{2(\theta_1 + \theta_2 - 2)c_t - \theta_*(\theta_2 - 1)}{(\theta_1 + \theta_2 - 1)(\theta_1 + \theta_2 - 2)}.$$
 (9)

After inserting (8) into (4), we can define η as a function of the parameters of the CHE, namely $\{\theta_k\}$, t and c_t . One also needs to solve the zero condition of the tau function, i.e. equation (3a), which, up to an elementary function, can be written in terms of a determinant of an integral operator K [58, 66]:

$$\det(\mathbb{1} - \mathsf{K}(\{\theta_k\}; c_t, t)) = 0. \tag{10}$$

For the sake of the argument, we assume that K has finite rank and can thus be represented as a matrix in an appropriate basis. In our application, the parameters of the equation above are functions of $M\omega$, a/M and $M\mu$, for fixed quantum numbers ℓ, m (we assume that the angular eigenvalue problem has been solved). We thus arrive at a working definition $\mathsf{K} = \mathsf{K}(M\omega, a/M, M\mu)$.

At a generic point in the parameter space, the determinant has isolated zeros in $M\omega$, which correspond to QNM frequencies. A given change of a/M or $M\mu$ produces a change in the QNM frequency. Linearization of (10) implies that the variations $\delta(M\omega)$, $\delta(a/M)$, and $\delta(M\mu)$ are related by

$$K_{M\omega}\delta(M\omega) + K_{a/M}\delta(a/M) + K_{M\mu}\delta(M\mu) = 0, \quad (11)$$

where

$$K_X = \text{Tr}\left[\text{adj}(\mathbb{1} - \mathsf{K})\frac{\partial \mathsf{K}}{\partial X}\right],$$
 (12)

with $X = \{M\omega, a/M, M\mu\}$. The adjugate adj A of a matrix A is the transpose of the matrix of cofactors

and, for invertible matrices, is related to the inverse by $adj(A) = det(A) A^{-1}$. Unlike the inverse, however, the adjugate is well-defined even when det A = 0.

We assume that the existence of an EP is due to a double zero of (10), meaning that the associated QNM frequecies are doubly degenerate. In this case, the linearization (11) is not enough to describe infinitesimal changes, and we have to consider higher order terms in the expansion. This means that, at an EP, the following condition is satisfied.

$$K_{M\omega} = \text{Tr}\left[\text{adj}(\mathbb{1} - \mathsf{K})\frac{\partial \mathsf{K}}{\partial (M\omega)}\right] = 0.$$
 (13)

In addition, near an EP, the linearization (11) must be replaced by

$$K'_{M\omega}(\delta(M\omega))^2 + K_{a/M}\delta(a/M) + K_{M\mu}\delta(M\mu) = 0, (14)$$
where

$$K'_{M\omega} = -\frac{1}{2} \operatorname{Tr} \left[\operatorname{adj}(\mathbb{1} - \mathsf{K}) \frac{\partial \mathsf{K}}{\partial (M\omega)} \right]^{2} - \frac{1}{2} \operatorname{Tr} \left[\operatorname{adj}(\mathbb{1} - \mathsf{K}) \frac{\partial^{2} \mathsf{K}}{\partial (M\omega)^{2}} \right]. \quad (15)$$

Note that (14) is equivalent to (5). In particular, the coefficients A_n and B_n of (5) take the form

$$A_n = \frac{K_{a/M}}{K'_{M\omega}}, \qquad B_n = \frac{K_{M\mu}}{K'_{M\omega}}, \tag{16}$$

where the expressions on the right hand side must be evaluated at the EP indexed by the integer n, i.e. $((M\omega)_n^c, (a/M)_n^c, (M\mu)_n^c)$. These quantities can, in principle, be computed by truncating K and using the Cayley-Hamilton theorem to express the adjugate in terms of a polynomial in K, but the process is computationally demanding. Instead, we fit (5) to the numerical data, as shown in Table II.

The behavior of the coefficients A_n is particularly interesting. In Fig. 5, we show the real and imaginary parts of A_n as a function of n. Both series of data in Table II are well fitted by harmonic sequencies of the form $\alpha/(n+\beta)$, with $(\alpha,\beta)=(7.721\times 10^{-4},0.647)$ fitting the data for $\operatorname{Re}(A_n)$ and $(\alpha,\beta)=(-7.796\times 10^{-4},0.970)$ fitting the data for $\operatorname{Im}(A_n)$. In particular, these fits suggest that there is an infinite number of EPs, and that, in the limit $n\to\infty$, the coefficient A_n associated with the n-th EP tends to zero.

Extremal Kerr and the τ_{III} -function – For given values of the angular quantum numbers $\ell, m > 0$, the imaginary part of a QNM frequency may or may not vanish at the extremal point a/M = 1, characterizing a ZDM or a DM, respectively. In terms of the parameters of the CHE (1), extremality corresponds to the confluent limit:

$$\Lambda = \frac{1}{2}(\theta_2 + \theta_1), \quad \theta_0 = \theta_2 - \theta_1, \quad x = \Lambda z, \quad u = \Lambda t,$$
(17)

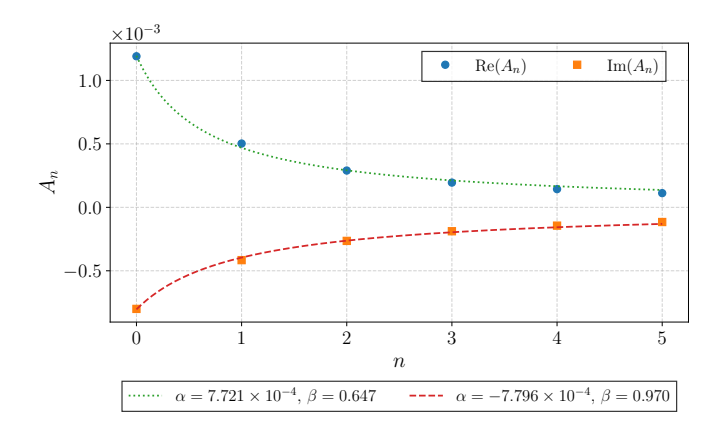


FIG. 5. The real (circle dots) and imaginary (square dots) parts of the coefficient A_n as a function of n, as given in Table II – see also Eqs. (5) and (16). The dashed and dotted lines correspond, respectively, to fits of $Re(A_n)$ and $Im(A_n)$ with respect to an harmonic sequence of the form $\alpha/(n+\beta)$.

with $\Lambda \to \infty$. This brings (1) to the form

$$\frac{d^{2}h}{dx^{2}} + \left[\frac{2-\theta_{\circ}}{x} - \frac{u}{x^{2}}\right] \frac{dh}{dx} - \left[\frac{1}{4} + \frac{\theta_{\star}}{2x} + \frac{uc_{u} - u/2}{x^{2}}\right] h = 0,$$
(18)

with $uc_u = \lim_{\Lambda \to \infty} tc_t$. The equation above is the double-confluent Heun equation (DCHE), an ordinary differential equation with two irregular singularities of Poincaré rank 1 at z = 0 and $z = \infty$ [82].

We have to solve simultaneously the angular and radial eigenvalue problems to determine QNMs. The angular problem has a smooth extremal limit and, hence, even in the case of extremal black holes can be formulated using the Painlevé V transcendent (3) [58]. In particular, the angular eigenvalue $\lambda_{\ell,m}$ can be expanded as

$$\lambda_{\ell,m} = \ell(\ell+1) - \frac{\left(2\ell(\ell+1) - 2m^2 - 1\right)}{4\ell(\ell+1) - 3} M^2 \left(\omega^2 - \mu^2\right) + \mathcal{O}(M^4(\omega^2 - \mu^2)^2).$$
 (19)

The analysis of the radial equation, on the other hand, is more involved. The parameter Λ in this case can be expanded, near extremality, as

$$\Lambda = \frac{i(2M\omega - m)}{\delta} + \frac{1}{3}i\delta(m + M\omega) + \mathcal{O}(\delta^2), \quad (20)$$

with δ defined through $a/M=\cos\delta$ (when $\delta=0,\,a/M=1$ and the black hole is extremal). We then see that Λ diverges in the extremal limit unless $M\omega\to m/2$, which is the case for DMs. The corresponding parameters for the radial DCHE are

$$\theta_{\circ} = 4iM\omega, \qquad \theta_{\star} = i\frac{2M(2\omega^2 - \mu^2)}{\sqrt{\omega^2 - \mu^2}}.$$
 (21)

Moreover, the accessory parameter c_u and the modulus

u are:

$$u = 4M(m - 2M\omega)\sqrt{\omega^2 - \mu^2},$$
 (22a)

$$u c_u = \lambda_{l,m} + \frac{1}{2}u + M^2(\mu^2 - 7\omega^2) - \frac{1}{4}(\theta_{\star} - 2)\theta_{\star}.$$
 (22b)

As discussed in [61], the Riemann-Hilbert map for the DCHE is written in terms of the tau function for the Painlevé III transcendent as

$$\tau_{III}(\theta_{\star}, \theta_{\circ}; \sigma, \eta; u) = 0,$$

$$\frac{d}{du} \log \tau_{III}(\theta_{\star} - 1, \theta_{\circ} - 1; \sigma - 1, \eta; u) - \frac{(\theta_{\circ} - 1)^{2}}{2u} = c_{u},$$
(23)

where σ and η are monodromy parameters that play essentially the same role as their non-confluent counterparts when $0 \leq a/M < 1$. Small u expansions for η and c_u as functions of $\theta_{\star}, \theta_{\circ}$, and σ are available in [61]. For a more comprehensive review of the mathematical framework of (23), we also refer the reader to [64].

We assume $\text{Re}(M\omega) \geq m/2$, ensuring that Λ diverges in the upper half-plane as $\delta \to 0$. Since $\text{Im}(M\omega) < 0$, this divergence occurs in the first quadrant. Under this assumption, the QNM condition (4) in the extremal limit reduces to

$$e^{i\pi\eta} = e^{-2\pi i\sigma} \frac{\sin\frac{\pi}{2}(\theta_{\star} + \sigma)}{\sin\frac{\pi}{2}(\theta_{\star} - \sigma)} \frac{\sin\frac{\pi}{2}(\theta_{\circ} + \sigma)}{\sin\frac{\pi}{2}(\theta_{\circ} - \sigma)}.$$
 (24)

Using the Riemann-Hilbert map (23) and the quantization condition (24), we determine the DMs associated with the extremal spin a/M=1. In the restricted domain $\text{Re}(M\omega) \geq m/2$, and focusing on the cases $(\ell,m)=(1,1)$ and (2,2), we find that the correct QNM flux conditions at both the outer horizon and infinity are satisfied only for $(M\mu)_c^* \leq M\mu \leq M\mu_{\text{max}}$. Within this mass range, the resulting solutions are DMs. As a further consistency check, we then followed these DMs adiabatically for a/M < 1, down to the origin of the parameter space, and verified that they coincide with modes in the Schwarzschild overtone spectrum.

We have also investigated the existence of modes with $\text{Re}(M\omega) < m/2$. By tracking the corresponding solutions throughout the parameter space, we found that they fail to reproduce known QNMs in the limit $a/M \to 0$. A closer examination of these spurious solutions shows that they do not satisfy the standard QNM flux conditions at either the outer horizon or at infinity.

^{*} joao.cavalcante@ufabc.edu.br

[†] mauricio.richartz@ufabc.edu.br

[‡] bruno.ccunha@ufpe.br

^[1] E. S. C. Ching, P. T. Leung, A. Maassen van den Brink, W. M. Suen, S. S. Tong, and K. Young, Quasinormalmode expansion for waves in open systems, Rev. Mod. Phys. 70, 1545 (1998), arXiv:gr-qc/9904017.

- [2] K. D. Kokkotas and B. G. Schmidt, Quasinormal modes of stars and black holes, Living Rev. Rel. 2, 2 (1999), arXiv:gr-qc/9909058.
- [3] H.-P. Nollert, Quasinormal modes: the characteristic 'sound' of black holes and neutron stars, Class. Quant. Grav. 16, R159 (1999).
- [4] E. Berti, V. Cardoso, and A. O. Starinets, Quasinormal modes of black holes and black branes, Class. Quant. Grav. 26, 163001 (2009), arXiv:0905.2975 [gr-qc].
- [5] R. A. Konoplya and A. Zhidenko, Quasinormal modes of black holes: From astrophysics to string theory, Rev. Mod. Phys. 83, 793 (2011), arXiv:1102.4014 [gr-qc].
- [6] F. Alpeggiani, N. Parappurath, E. Verhagen, and L. Kuipers, Quasinormal-Mode Expansion of the Scattering Matrix, Physical Review X 7, 021035 (2017), arXiv:1609.03902 [physics.optics].
- [7] E. Berti *et al.*, Black hole spectroscopy: from theory to experiment, (2025), arXiv:2505.23895 [gr-qc].
- [8] M. J. Jacquet, L. Giacomelli, Q. Valnais, M. Joly, F. Claude, E. Giacobino, Q. Glorieux, I. Carusotto, and A. Bramati, Quantum Vacuum Excitation of a Quasinormal Mode in an Analog Model of Black Hole Spacetime, Phys. Rev. Lett. 130, 111501 (2023), arXiv:2110.14452 [gr-qc].
- [9] T. Torres, S. Patrick, M. Richartz, and S. Weinfurtner, Quasinormal Mode Oscillations in an Analogue Black Hole Experiment, Phys. Rev. Lett. 125, 011301 (2020), arXiv:1811.07858 [gr-qc].
- [10] C. V. Vishveshwara, Scattering of Gravitational Radiation by a Schwarzschild Black-hole, Nature 227, 936 (1970).
- [11] T. J. Zouros and D. M. Eardley, Instabilities of massive scalar perturbations of a rotating black hole, Annals of Physics 118, 139 (1979).
- [12] M. Davis, R. Ruffini, W. H. Press, and R. H. Price, Gravitational radiation from a particle falling radially into a schwarzschild black hole, Phys. Rev. Lett. 27, 1466 (1971).
- [13] B. P. Abbott *et al.* (LIGO Scientific, Virgo), Observation of Gravitational Waves from a Binary Black Hole Merger, Phys. Rev. Lett. **116**, 061102 (2016), arXiv:1602.03837 [gr-qc].
- [14] F. Echeverria, Gravitational Wave Measurements of the Mass and Angular Momentum of a Black Hole, Phys. Rev. D 40, 3194 (1989).
- [15] O. Dreyer, B. J. Kelly, B. Krishnan, L. S. Finn, D. Garrison, and R. Lopez-Aleman, Black hole spectroscopy: Testing general relativity through gravitational wave observations, Class. Quant. Grav. 21, 787 (2004), arXiv:gr-qc/0309007.
- [16] E. Berti, A. Sesana, E. Barausse, V. Cardoso, and K. Belczynski, Spectroscopy of Kerr black holes with Earthand space-based interferometers, Phys. Rev. Lett. 117, 101102 (2016), arXiv:1605.09286 [gr-qc].
- [17] H. Yang, F. Zhang, A. Zimmerman, D. A. Nichols, E. Berti, and Y. Chen, Branching of quasinormal modes for nearly extremal Kerr black holes, Phys. Rev. D 87, 041502 (2013), arXiv:1212.3271 [gr-qc].
- [18] H. Yang, A. Zimmerman, A. Zenginoğlu, F. Zhang, E. Berti, and Y. Chen, Quasinormal modes of nearly extremal Kerr spacetimes: spectrum bifurcation and power-law ringdown, Phys. Rev. D 88, 044047 (2013), arXiv:1307.8086 [gr-qc].
- [19] H. Yang, A. Zimmerman, and L. Lehner, Turbulent

- Black Holes, Phys. Rev. Lett. **114**, 081101 (2015), arXiv:1402.4859 [gr-qc].
- [20] S. E. Gralla, A. Zimmerman, and P. Zimmerman, Transient Instability of Rapidly Rotating Black Holes, Phys. Rev. D 94, 084017 (2016), arXiv:1608.04739 [gr-qc].
- [21] M. Casals, S. E. Gralla, and P. Zimmerman, Horizon Instability of Extremal Kerr Black Holes: Nonaxisymmetric Modes and Enhanced Growth Rate, Phys. Rev. D 94, 064003 (2016), arXiv:1606.08505 [gr-qc].
- [22] M. Richartz, C. A. R. Herdeiro, and E. Berti, Synchronous frequencies of extremal Kerr black holes: resonances, scattering and stability, Phys. Rev. D 96, 044034 (2017), arXiv:1706.01112 [gr-qc].
- [23] M. Casals and L. F. Longo Micchi, Spectroscopy of extremal and near-extremal Kerr black holes, Phys. Rev. D 99, 084047 (2019), arXiv:1901.04586 [gr-qc].
- [24] R. Teixeira da Costa, Mode stability for the Teukolsky equation on extremal and subextremal Kerr spacetimes, Commun. Math. Phys. 378, 705 (2020), arXiv:1910.02854 [gr-qc].
- [25] S. Klainerman and J. Szeftel, Brief introduction to the nonlinear stability of Kerr, Pure Appl. Math. Quart. 20, 1721 (2024), arXiv:2210.14400 [math.AP].
- [26] Y. Shlapentokh-Rothman and R. T. da Costa, Boundedness and decay for the Teukolsky equation on Kerr in the full subextremal range |a| < M: physical space analysis, (2023), arXiv:2302.08916 [gr-qc].
- [27] T. Kato, Perturbation Theory for Linear Operators, Grundlehren der mathematischen Wissenschaften, Vol. 132 (Springer, 1995).
- [28] Y. Ashida, Z. Gong, and M. Ueda, Non-Hermitian physics, Adv. Phys. 69, 249 (2021), arXiv:2006.01837 [cond-mat.mes-hall].
- [29] M. Yang, L. Zhu, Q. Zhong, R. El-Ganainy, and P.-Y. Chen, Spectral sensitivity near exceptional points as a resource for hardware encryption, Nature Communications 14, 1145 (2023).
- [30] E. Cohen, H. Larocque, F. Bouchard, F. Nejadsattari, Y. Gefen, and E. Karimi, Geometric phase from Aharonov-Bohm to Pancharatnam-Berry and beyond, Nature Rev. Phys. 1, 437 (2019), arXiv:1912.12596 [quant-ph].
- [31] A. Davey, O. J. C. Dias, and J. E. Santos, Scalar QNM spectra of Kerr and Reissner-Nordström revealed by eigenvalue repulsions in Kerr-Newman, JHEP 12, 101, arXiv:2305.11216 [gr-qc].
- [32] O. J. C. Dias, M. Godazgar, and J. E. Santos, Eigenvalue repulsions and quasinormal mode spectra of Kerr-Newman: an extended study, JHEP 07, 076, arXiv:2205.13072 [gr-qc].
- [33] O. J. C. Dias, M. Godazgar, J. E. Santos, G. Carullo, W. Del Pozzo, and D. Laghi, Eigenvalue repulsions in the quasinormal spectra of the Kerr-Newman black hole, Phys. Rev. D 105, 084044 (2022), arXiv:2109.13949 [gr-qc].
- [34] H. Motohashi, Resonant Excitation of Quasinormal Modes of Black Holes, Phys. Rev. Lett. 134, 141401 (2025), arXiv:2407.15191 [gr-qc].
- [35] J. P. Cavalcante, M. Richartz, and B. C. da Cunha, Massive scalar perturbations in Kerr black holes: Near extremal analysis, Phys. Rev. D 110, 124064 (2024), arXiv:2408.13964 [gr-qc].
- [36] J. P. Cavalcante, M. Richartz, and B. C. da Cunha, Exceptional Point and Hysteresis in Perturbations of

- Kerr Black Holes, Phys. Rev. Lett. **133**, 261401 (2024), arXiv:2407.20850 [gr-qc].
- [37] M. Am-Shallem, R. Kosloff, and N. Moiseyev, Exceptional points for parameter estimation in open quantum systems: analysis of the bloch equations, New Journal of Physics 17, 113036 (2015), arXiv:1411.6364 [quant-ph].
- [38] H. Liu, Y. Li, Y. Zhang, J. Zhang, W. Zhang, J. Ren, H. Zhang, and Y. Zhang, Observation of exceptional points in magnonic parity-time symmetric systems, Science Advances 5, eaax9144 (2019).
- [39] M.-X. Shi, X. M. Su, and X.-L. Zhang, Encircling exceptional points in non-hermitian systems with quasidegenerate energy levels, Phys. Rev. A 105, 062214 (2022).
- [40] N. Oshita, E. Berti, and V. Cardoso, Unstable Chords and Destructive Resonant Excitation of Black Hole Quasinormal Modes, Phys. Rev. Lett. 135, 031401 (2025), arXiv:2503.21276 [gr-qc].
- [41] Y. Yang, E. Berti, and N. Franchini, Black Hole Quasinormal Mode Resonances, Phys. Rev. Lett. 135, 201401 (2025), arXiv:2504.06072 [gr-qc].
- [42] C. Chen, J. Jing, Z. Cao, and M. Wang, Complete quasinormal modes of type-D black holes, Phys. Rev. D 112, 103036 (2025), arXiv:2506.14635 [gr-qc].
- [43] R. K. L. Lo, L. Sabani, and V. Cardoso, Quasinormal modes and excitation factors of Kerr black holes, Phys. Rev. D 111, 124002 (2025), arXiv:2504.00084 [gr-qc].
- [44] G. Aminov, A. Grassi, and Y. Hatsuda, Black Hole Quasinormal Modes and Seiberg-Witten Theory, Annales Henri Poincare 23, 1951 (2022), arXiv:2006.06111 [hep-th].
- [45] G. Bonelli, C. Iossa, D. P. Lichtig, and A. Tanzini, Exact solution of Kerr black hole perturbations via CFT2 and instanton counting: Greybody factor, quasinormal modes, and Love numbers, Phys. Rev. D 105, 044047 (2022), arXiv:2105.04483 [hep-th].
- [46] D. Consoli, F. Fucito, J. F. Morales, and R. Poghossian, CFT description of BH's and ECO's: QNMs, superradiance, echoes and tidal responses, JHEP 12, 115, arXiv:2206.09437 [hep-th].
- [47] G. Bonelli, C. Iossa, D. Panea Lichtig, and A. Tanzini, Irregular Liouville Correlators and Connection Formulae for Heun Functions, Commun. Math. Phys. 397, 635 (2023), arXiv:2201.04491 [hep-th].
- [48] O. Lisovyy and A. Naidiuk, Perturbative connection formulas for Heun equations, J. Phys. A 55, 434005 (2022), arXiv:2208.01604 [math-ph].
- [49] M. Ablowitz and H. Segur, Solitons and the Inverse Scattering Transform, Studies in Applied and Numerical Mathematics (Society for Industrial and Applied Mathematics, 2006).
- [50] A. Its and V. Novokshenov, The Isomonodromic Deformation Method in the Theory of Painleve Equations, Lecture Notes in Mathematics (Springer Berlin Heidelberg, 2006).
- [51] M. Jimbo, T. Miwa, and A. K. Ueno, Monodromy Preserving Deformation of Linear Ordinary Differential Equations With Rational Coefficients, I, Physica D2, 306 (1981).
- [52] M. Jimbo and T. Miwa, Monodromy Preserving Deformation of Linear Ordinary Differential Equations with Rational Coefficients, II, Physica D2, 407 (1981).
- [53] M. Jimbo and T. Miwa, Monodromy Preserving Deformation of Linear Ordinary Differential Equations with Rational Coefficients, III, Physica D4, 26 (1981).

- [54] O. Gamayun, N. Iorgov, and O. Lisovyy, How instanton combinatorics solves Painlevé VI, V and IIIs, J. Phys. A 46, 335203 (2013), arXiv:1302.1832 [hep-th].
- [55] F. Novaes and B. Carneiro da Cunha, Isomonodromy, Painlevé transcendents and scattering off of black holes, JHEP 07, 132, arXiv:1404.5188 [hep-th].
- [56] B. Carneiro da Cunha and F. Novaes, Kerr Scattering Coefficients via Isomonodromy, JHEP 11, 144, arXiv:1506.06588 [hep-th].
- [57] F. Novaes, C. Marinho, M. Lencsés, and M. Casals, Kerr-de Sitter Quasinormal Modes via Accessory Parameter Expansion, JHEP 05, 033, arXiv:1811.11912 [gr-qc].
- [58] B. Carneiro da Cunha and J. a. P. Cavalcante, Confluent conformal blocks and the Teukolsky master equation, Phys. Rev. D102 (2020), arXiv:1906.10638 [hep-th].
- [59] J. B. Amado, B. Carneiro da Cunha, and E. Pallante, Vector perturbations of Kerr-AdS₅ and the Painlevé VI transcendent, JHEP 04, 155, arXiv:2002.06108 [hep-th].
- [60] B. Carneiro da Cunha and J. P. Cavalcante, Teukolsky master equation and Painlevé transcendents: Numerics and extremal limit, Phys. Rev. D 104, 084051 (2021), arXiv:2105.08790 [hep-th].
- [61] J. P. Cavalcante and B. Carneiro da Cunha, Scalar and Dirac perturbations of the Reissner-Nordström black hole and Painlevé transcendents, Phys. Rev. D 104, 124040 (2021), arXiv:2109.06929 [gr-qc].
- [62] J. B. Amado, B. C. da Cunha, and E. Pallante, Quasinormal modes of scalar fields on small Reissner-Nordström-AdS5 black holes, Phys. Rev. D 105, 044028 (2022), arXiv:2110.08349 [hep-th].
- [63] B. Carneiro da Cunha and J. P. Cavalcante, Expansions for semiclassical conformal blocks, Journal of High Energy Physics 08, 110 (2024), arXiv:2211.03551 [hep-th].
- [64] J. P. Cavalcante, Isomonodromy method and black holes quasinormal modes: numerical results and extremal limit analysis (2023), arXiv:2307.16209 [hep-th].
- [65] J. P. Cavalcante, M. Richartz, and B. Carneiro da Cunha, Data and scripts for: Exceptional point and hysteresis in perturbations of kerr black holes and massive scalar perturbations in kerr black holes: near extremal analysis, 10.5281/zenodo.13961216 (2024).
- [66] O. Lisovyy, H. Nagoya, and J. Roussillon, Irregular conformal blocks and connection formulae for Painlevé V functions, J. Math. Phys. 59, 091409 (2018), arXiv:1806.08344 [math-ph].
- [67] S. Hod, Quasinormal resonances of a massive scalar field in a near-extremal Kerr black hole spacetime, Phys. Rev. D 84, 044046 (2011), arXiv:1109.4080 [gr-qc].
- [68] S. Hod, Slow relaxation of rapidly rotating black holes, Phys. Rev. D 78, 084035 (2008), arXiv:0811.3806 [gr-qc].
- [69] S. Detweiler, Black holes and gravitational waves. III -The resonant frequencies of rotating holes, Astrophys. J. 239, 292 (1980).
- [70] V. Cardoso, A Note on the resonant frequencies of rapidly rotating black holes, Phys. Rev. D 70, 127502 (2004), arXiv:gr-qc/0411048.
- [71] L. Motl, An Analytical computation of asymptotic Schwarzschild quasinormal frequencies, Adv. Theor. Math. Phys. 6, 1135 (2003), arXiv:gr-qc/0212096.
- [72] A. Neitzke, Greybody factors at large imaginary frequencies, (2003), arXiv:hep-th/0304080.
- [73] A. Maassen van den Brink, WKB analysis of the Regge-Wheeler equation down in the frequency plane, J. Math. Phys. 45, 327 (2004), arXiv:gr-qc/0303095.

- [74] S. Musiri and G. Siopsis, Perturbative calculation of quasinormal modes of Schwarzschild black holes, Class. Quant. Grav. 20, L285 (2003), arXiv:hep-th/0308168.
- [75] J. Doppler, A. A. Mailybaev, J. Böhm, U. Kuhl, A. Girschik, F. Libisch, T. J. Milburn, P. Rabl, N. Moiseyev, and S. Rotter, Dynamically encircling an exceptional point for asymmetric mode switching, Nature 537, 76 (2016), arXiv:1603.02325 [physics.optics].
- [76] A. U. Hassan, B. Zhen, M. Soljačić, M. Khajavikhan, and D. N. Christodoulides, Dynamically encircling exceptional points: Exact evolution and polarization state conversion, Phys. Rev. Lett. 118, 093002 (2017), arXiv:1706.09938 [physics.optics].
- [77] H. Zhao, X. Qiao, T. Wu, B. Midya, S. Longhi, and L. Feng, Non-hermitian topological light steering, Science 365, 1163 (2019).
- [78] Q. Liu, S. Li, B. Wang, S. Ke, C. Qin, K. Wang, W. Liu, D. Gao, P. Berini, and P. Lu, Efficient mode transfer on a compact silicon chip by encircling moving exceptional points, Phys. Rev. Lett. 124, 153903 (2020).

- [79] Y. S. S. Patil, J. Höller, P. A. Henry, C. Guria, Y. Zhang, L. Jiang, N. Kralj, N. Read, and J. G. E. Harris, Measuring the knot of non-Hermitian degeneracies and non-commuting braids, Nature 607, 271 (2022), arXiv:2112.00157 [physics.optics].
- [80] D. Long, X. Mao, G.-Q. Qin, H. Zhang, M. Wang, G.-Q. Li, and G.-L. Long, Dynamical encircling of the exceptional point in a largely detuned multimode optomechanical system, Phys. Rev. A 106, 053515 (2022), arXiv:2208.01228 [physics.optics].
- [81] C. Guria, Q. Zhong, S. K. Ozdemir, Y. S. S. Patil, R. El-Ganainy, and J. G. E. Harris, Resolving the topology of encircling multiple exceptional points, Nature Commun. 15, 1369 (2024), arXiv:2304.03207 [physics.optics].
- [82] DLMF, NIST Digital Library of Mathematical Functions (Chapter 13), http://dlmf.nist.gov/, Release 1.1.2 of 2021-06-15, f. W. J. Olver, A. B. Olde Daalhuis, D. W. Lozier, B. I. Schneider, R. F. Boisvert, C. W. Clark, B. R. Miller, B. V. Saunders, H. S. Cohl, and M. A. McClain, eds.